

# Simulation of free falling rigid body into water by a stabilized incompressible SPH method

Abdelraheem M. Aly\*, Mitsuteru Asai and Yoshimi Sonoda

*Civil Engineering Department, Faculty of Engineering, Kyushu University, Japan*

*(Received May 12, 2011, Accepted July 28, 2011)*

**Abstract.** A stabilized incompressible smoothed particles hydrodynamics (ISPH) method is utilized to simulate free falling rigid body into water domain. Both of rigid body and fluid domain are modeled by SPH formulation. The proposed source term in the pressure Poisson equation contains two terms; divergence of velocity and density invariance. The density invariance term is multiplied by a relaxed parameter for stabilization. In addition, large eddy simulation with Smagorinsky model has been introduced to include the eddy viscosity effect. The improved method is applied to simulate both of free falling vessels with different materials and water entry-exit of horizontal circular cylinder. The applicability and efficiency of improved method is tested by the comparisons with reference experimental results.

**Keywords:** incompressible SPH; rigid body; free surface flow; pressure Poisson equation.

---

## 1. Introduction

The accurate prediction of impact loads by fluid provides important information on the safety of ships and has many applications in scientific and engineering computations, e.g., aerodynamic around an air craft and debris motion in a flood. Numerous experimental, theoretical and numerical studies have been performed to study the water entry problems. Greenhow and Lin (1983) conducted a series of experiments to show the considerable differences in the free surface deformation for the entry and exit of a circular cylinder. Zhao *et al.* (1997) used both the experiment and the potential flow theory to investigate the water entry of a falling wedge. Similar water entry problems have also been studied by Tyvand and Miloh (1995) using a series expansion approach and by Greenhow and Moyo (1997) using a non-linear boundary element method model based on the irrotational flow assumption.

The large deformation and violent behavior of coupled free surface with impact loads by liquid sloshing, is the most difficult problem for numerical simulations because the implementation of the fully nonlinear free-surface condition is in general complicated. There are several techniques to handle such problems. Hirt and Nichols (1981) used a simple method to approximate free boundaries in finite difference numerical simulations, based on the concept of a fractional volume of fluid (SOLA-VOF). Sussman *et al.* (1994) presented a level set approach for computing solutions to incompressible two-phase flow. Marker density function (MDF) is introduced by Miyata and Park

---

\*Corresponding author, Ph.D. candidate, E-mail: [abdelraheem@doc.kyushu-u.ac.jp](mailto:abdelraheem@doc.kyushu-u.ac.jp)

(1995). Kleefsman *et al.* (2005) and Panahi *et al.* (2006) computed the water entry of a cylinder by solving the N–S equation with a volume-of-fluid surface tracking using a finite volume formulation. Lin (2007) used the concept of a locally relative stationary in his Reynolds-averaged N–S (RANS) modeling to study the water entry of a circular cylinder with prescribed falling velocity. Most of the previous techniques are capturing the free-surface on grid system. However, there is a different approach without grid system, the so-called particle methods, which provides a robust numerical tool to simulate the complicated interactions between the flow and a solid body. Owing to the mesh-free nature, the breakup and reconnection of the free surfaces can be easily realized in a particle method without the sophisticated mesh management as required in a grid method. The capability of the particle model has been evidenced in the simulations of breaking wave impact on a moving float by Koshizuka *et al.* (1998) and Gotoh and Sakai (2006) using the moving particle semi-implicit (MPS) method. Recently, Lee *et al.* (2010) are introduced moving particle semi-implicit (MPS) method to simulate violent free-surface motions interacting with structures. On the other hand, the smoothed particle hydrodynamic (SPH) method was originally proposed by Lucy (1977) and further developed by Gingold and Monaghan (1977) for treating astrophysical problems. Its main advantage is the absence of a computational grid or mesh since it is spatially discretized into Lagrangian moving particles. This allows the possibility of easily modeling flows with a complex geometry or flows where large deformations or the appearance of a free surface occurs. Oger *et al.* (2006) employed the 2D SPH model with a fluid–solid coupling technique to study the water entry of a wedge with different degrees of freedom. The numerical model used a highly robust spatially varying particle resolution to improve the computational accuracy and efficiency. Recently, Liu *et al.* (2009) implemented the two phase SPH model to simulate water entry of a wedge. The SPH is originally developed in compressible flow, and then some special treatment is required to satisfy the incompressible condition. Shao and Lo (2003) introduced an incompressible version of the SPH. In incompressible SPH method, the pressure is implicitly calculated by solving a discretized pressure Poisson equation at every time step. Lee *et al.* (2006) showed that, the incompressible SPH model able to realistically predict the pressure field of the flows due to its hydrodynamic formulations. Recently, an incompressible SPH model had been widely used to simulate free surface flows for incompressible fluids (Ellero *et al.* 2007, Lee *et al.* 2008, Khayyer *et al.* 2008, Khayyer *et al.* 2009). Lee *et al.* (2008) presented comparisons of a semi-implicit and truly incompressible SPH (ISPH) algorithm with the classical WCSPH method, showing how some of the problems encountered in WCSPH have been resolved by using ISPH to simulate incompressible flows. He used the function of temporal velocity divergence for discretized source terms of Poisson equation of pressure to ensure truly incompressible flow. Khayyer *et al.* (2008, 2009) proposed a corrected incompressible SPH method (CISPH) derived based on a variational approach to ensure the angular momentum conservation of ISPH formulations to improve the pressure distribution by improvement of momentum conservation and the second improvement is achieved by deriving and employing a higher order source term based on a more accurate differentiation.

In this paper, stabilized incompressible smoothed particle hydrodynamics is introduced to simulate both of free falling vessels with different manufacturing materials and water entry-exit of circular cylinder. The density invariance in the pressure Poisson equation multiplies by a relaxed parameter for more stabilization. The comparison between the proposed ISPH model and experimental results as Greenhow and Lin (1983) for water entry and exit of circular cylinder has been introduced and it showed a good agreement. The proposed model showed adjustment in free surface deformation and keeping the total volume of fluid during the whole simulation.

## 2. Mathematical analysis

In this section, the governing equation for the current method is introduced and description of the method is discussed in details.

### 2.1 Governing equations

The mass and momentum equations of the incompressible flows are presented as

$$\nabla \cdot \bar{u} = 0 \quad (1)$$

$$\frac{D\bar{u}}{Dt} = -\frac{1}{\rho}\nabla p + \nu\nabla^2\bar{u} + \frac{1}{\rho}\nabla \cdot \dot{\tau} + \bar{F} \quad (2)$$

where  $\rho$  and  $\nu$  are density and kinematic viscosity of fluid,  $\bar{u}$  is the velocity vector and  $p$  is pressure,  $\bar{F}$  is external force, and  $t$  indicates time. In the most general incompressible flow approach, the density is assumed by a constant value with its initial value  $\rho^0$ . The main concept in an incompressible SPH method is solving a discretized pressure Poisson equation at every time step to get the pressure value. In this paper, we used the following equation for the pressure Poisson equation

$$\langle \nabla^2 P_i^{n+1} \rangle = \frac{\rho^0}{\Delta t} \langle \nabla \cdot \bar{u}_i^* \rangle + \alpha \frac{\rho^0 - \langle \rho_i^n \rangle}{\Delta t^2} \quad (3)$$

where, ( $0 \leq \alpha \leq 1$ ) is relaxation coefficient,  $\bar{u}^*$  is temporal velocity, triangle bracket  $\langle \rangle$  means SPH approximation, which is explained in the next section. Deriving Eq. (3) is proposed by Tanaka and Masunaga (2010) in the framework of MPS method.

### 2.2 SPH formulation

The fundamental basis of the SPH method is the interpolation theory. The method allows any function to be expressed in terms of its values at a set of disordered points representing particle positions using kernel function. A physical scalar function  $A(r)$  at a certain position  $r$  can be represented by the following integral form

$$A(r) = \int_V A(r') W(r-r', h) dr' \quad (4)$$

where  $V$  represents the solution space and the smoothing length  $h$  represents the effective width of the kernel. The properties of the kernel function should satisfy the following two conditions for mass and energy conservation

$$\int_V W(r-r', h) dr' = \lim_{h \rightarrow 0} W(r-r', h) = \delta(r-r') \quad (5)$$

For SPH numerical analysis, the integral Eq. (4) is approximated by a summation of contributions from neighbor particles in the support domain

$$A(r_i) = \langle A_i \rangle = \sum_j \frac{m_j}{\rho_j} W(r_{ij}, h) A_j(r_j, t) \quad (6)$$

where the subscripts  $i$  and  $j$  indicate positions of labeled particle, and  $m_j$  means representative mass related to particle  $j$ . The density  $\langle \rho_i^n \rangle$  in SPH form is defined by

$$\rho(x_i) \approx \langle \rho_i \rangle = \sum_j m_j W(r_{ij}, h) = \sum_j m_j W_{ij} \quad (7)$$

The gradient of the scalar function can be assumed by using the above defined SPH approximation as follows

$$\nabla A(r_i) \approx \langle \nabla A_i \rangle = \frac{1}{\rho_i} \sum_j m_j (A_j - A_i) \nabla W(r_{ij}, h) \quad (8)$$

Also, the other expression for the gradient can be represented by

$$\nabla A(r_i) \approx \langle \nabla A_i \rangle = \rho_i \sum_j m_j \left( \frac{A_j}{\rho_j^2} + \frac{A_i}{\rho_i^2} \right) \nabla W(r_{ij}, h) \quad (9)$$

In this paper, quintic spline function is utilized as a kernel function for two-dimensional problems.

$$W(r_{ij}, h) = \frac{7}{478\pi h^2} \begin{cases} \left[ \left(3 - \frac{r_{ij}}{h}\right)^5 - 6\left(2 - \frac{r_{ij}}{h}\right)^5 + 15\left(1 - \frac{r_{ij}}{h}\right)^5 \right] & 0 \leq r_{ij} \leq h \\ \left[ \left(3 - \frac{r_{ij}}{h}\right)^5 - 6\left(2 - \frac{r_{ij}}{h}\right)^5 \right] & h \leq r_{ij} \leq 2h \\ \left[ \left(3 - \frac{r_{ij}}{h}\right)^5 \right] & 2h \leq r_{ij} \leq 3h \\ 0 & r_{ij} \geq 3h \end{cases} \quad (10)$$

In the current incompressible SPH method, the gradient of pressure and the divergence of velocity are approximated as follow

$$\nabla P(r_i) \approx \langle \nabla P_i \rangle = \rho_i \sum_j m_j \left( \frac{P_j}{\rho_j^2} + \frac{P_i}{\rho_i^2} \right) \nabla W(r_{ij}, h) \quad (11)$$

$$\nabla \cdot \bar{u}(r_i) \approx \langle \nabla \bar{u}_i \rangle = \frac{1}{\rho_i} \sum_j m_j (\bar{u}_j - \bar{u}_i) \cdot \nabla W(r_{ij}, h) \quad (12)$$

Although the Laplacian could be derived directly from the original SPH approximation of a function in Eq. (9), this approach may lead to a loss of resolution. Then, the second derivative of the laminar viscous force and the Laplacian of pressure have been proposed by Morris *et al.* (1997) by an approximation expression as follows

$$\nabla \cdot (\nu \nabla \bar{u})(x_i) \approx \langle \nabla \cdot (\nu \nabla \bar{u}_i) \rangle = \sum_j m_j \left( \frac{\rho_i \nu_i + \rho_j \nu_j}{\rho_i \rho_j} \frac{\bar{r}_{ij} \cdot \nabla W(|r - r_j|, h)}{r_{ij}^2 + \eta^2} \right) \bar{u}_{ij} \quad (13)$$

where  $\eta$  is a parameter to avoid a zero dominator, and its value is usually given by  $\eta^2 = 0.0001 h^2$ . Similarly, the Laplacian of pressure in pressure Poisson equation (PPE)

$$\nabla^2 P(x_i) \approx \langle \nabla^2 P_i \rangle = \frac{2}{\rho_i} \sum_j m_j \left( \frac{P_{ij} \bar{r}_{ij} \cdot \nabla W(|r_i - r_j|, h)}{r_{ij}^2 + \eta^2} \right) \quad (14)$$

The PPE after SPH interpolation is solved by a preconditioned (diagonal scaling) Conjugate Gradient (PCG) method with a convergence tolerance ( $=1.0 \times 10^{-9}$ ).

The SPS stress tensor is modeled through the traditional Boussinesq eddy viscosity assumption as

$$\tau_{ab}/\rho = 2\nu_T \bar{S}_{ab} - \frac{2}{3} k \delta_{ab} \quad (15)$$

where  $\nu_T$  is an eddy viscosity is calculated by using standard Smagorinsky model

$$\nu_T = (C_s \Delta)^2 |\bar{S}| \quad (16)$$

in which,  $C_s = 0.2$  is Smagorinsky constant,  $\Delta$  is constant and it taken as smoothing compact support  $3h$  in this scheme. The local strain rate  $|\bar{S}|$  is calculated as Violeau and Issa (2007). The turbulent kinetic energy  $k$  incorporated in the pressure term, and then the current viscous term is reformulated as follows

$$\langle \nabla \cdot (\nu_e \nabla \cdot \bar{u}_i) \rangle = \sum_j m_j \left( \frac{\rho_i \nu_{e,i} + \rho_j \nu_{e,j}}{\rho_i \rho_j} \bar{r}_{ij} \cdot \nabla W(|r_i - r_j|, h) \right) \bar{u}_{ij} \quad (17)$$

where  $\nu_{e,i} = \nu_i + \nu_{T,i}$ . Note that, the improved ISPH method includes the proposed source term in the pressure Poisson equation and the eddy viscosity effect, while the original ISPH method use the source term as divergence of velocity only ( $\alpha = 0$ ) without the eddy viscosity.

### 2.3 Treatment of moving rigid body

Koshizuka and Oka (1996) proposed a passively moving-solid model to describe the motion of rigid body in a fluid. Firstly, both of fluid and solid particles are solved with the same calculation procedures. Secondly, an additional procedure is applied to solid particles as follows: Assuming that, the number of solid particles is  $n$  with location  $\bar{r}_k$  for each particle, the centre of the solid object at  $\bar{r}_c$ , the relative coordinate of a solid particle to the centre  $\bar{q}_k$  and the moment of inertia  $I$  of the solid object are calculated by

$$\bar{r}_c = \frac{1}{n} \sum_{k=1}^n \bar{r}_k \quad (18)$$

$$\bar{q}_k = \bar{r}_k - \bar{r}_c \quad (19)$$

$$I = \sum_{k=1}^n |\bar{q}_k|^2 \quad (20)$$

The translational velocity  $\bar{T}$  and rotational velocity  $\bar{R}$  of solid object are calculated by

$$\bar{T} = \frac{1}{n} \sum_{k=1}^n \bar{u}_k \quad (21)$$

$$\bar{\mathbf{R}} = \frac{1}{I} \sum_{k=1}^n \bar{\mathbf{u}}_k \times \bar{\mathbf{q}}_k \quad (22)$$

Finally, the velocity of each particle in the solid body is replaced by

$$\bar{\mathbf{u}}_k = \bar{\mathbf{T}} + \bar{\mathbf{q}}_k \times \bar{\mathbf{R}} \quad (23)$$

From the above rigid body corrections, the motion of free moving object can be tracked as a complete rigid body. Gotoh and Sakai (2006) show that the previous treatment works very well in a stable computation where the Courant condition is satisfied. In addition, Shao (2009) investigated the water entry of a free falling wedge using an incompressible smoothed particles hydrodynamics (Incom-SPH).

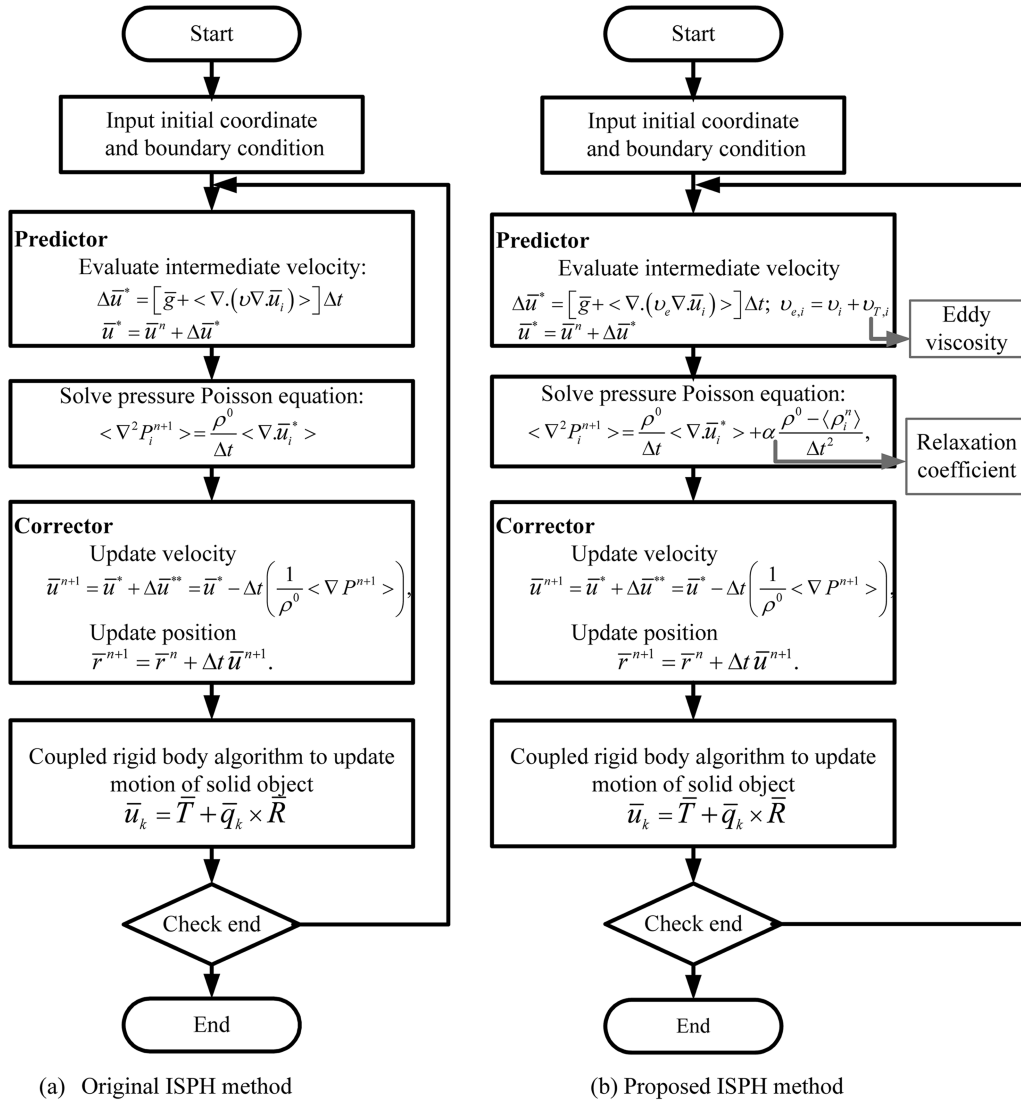


Fig. 1 Flowchart of (a) original ISPH and (b) proposed ISPH

## 2.4 Boundary condition

The boundary condition on the rigid bodies has an important role to prevent penetration and to reduce error related to truncation of the kernel function. In the current work, dummy particles technique, in which dummy particles are regularly distributed at the initial state and have zero velocity through the whole simulation process. Moreover, the pressure Poisson equation is solved for all particles including these dummy particles to get an enough repulsive force for preventing penetration.

## 3. Results and discussions

Numerical examples have been introduced to validate the current scheme.

### 3.1 Prediction of free falling vessels with different materials

In this section, the improved model has been used to simulate free falling vessels with different manufacturing materials and wood. The relaxation coefficient in the current simulation is taken as ( $\alpha = 0.15$ ), particle size is 1 cm and the time step  $\Delta t = 0.001$  s. The vessel is falling into liquid in tank; splash is appear from liquid and the vessel start floating. Note, the liquid in tank is taken as water with density  $\rho_f = 1.0 \text{ g/cm}^3$ . In the floating case, the position of vessel depends on the vessel material. Three different vessel materials in this simulation have been performed as shown in table 1. Fig. 2 shows the schematic diagram for the free falling vessel. The snapshots for the time

Table 1. Show the density of different vessel material

| Solid         | Density $\rho_s \text{ g/cm}^3$ |
|---------------|---------------------------------|
| Polypropylene | 0.86                            |
| Nylon         | 1.14                            |
| Delrin        | 1.41                            |

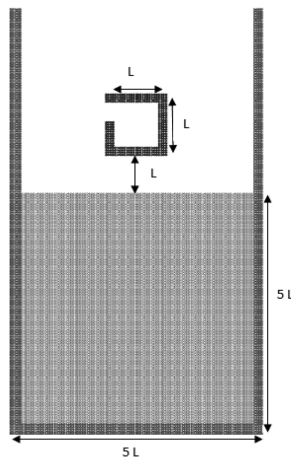


Fig. 2 Present the schematic diagram for the free falling vessel

history of floating vessel have been shown in Figs. 3-5. It is seen, as expected, that the vessel is floating and it still over the liquid in all times when the density ratio between the density of vessel and density of liquid is less than 1.0, while the vessel is floating until it fills completely by liquid when the density ratio is approximately equals to 1.0. In the third case, the density ratio is greater than 1.0, the vessel is rapidly falls down as the times goes and it fills completely by the liquid. Fig. 6 show the pressure distribution for free falling of three vessels during the simulation. It is observed that, the pressure distributions during the whole simulation are smooth. Finally, the current simulation shows a good agreement with the expected results and it keeps the total volume of fluid

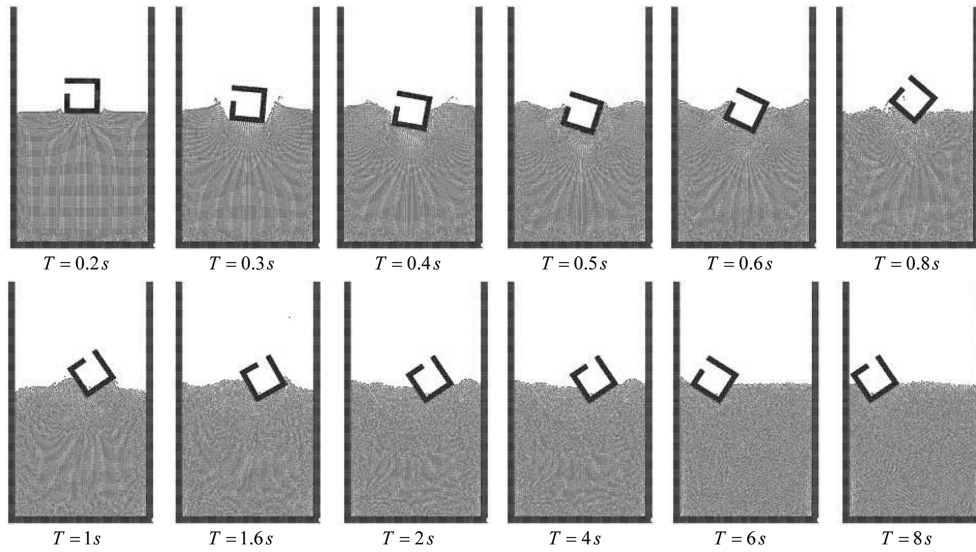


Fig. 3 Show time history for free falling of Polypropylene vessel

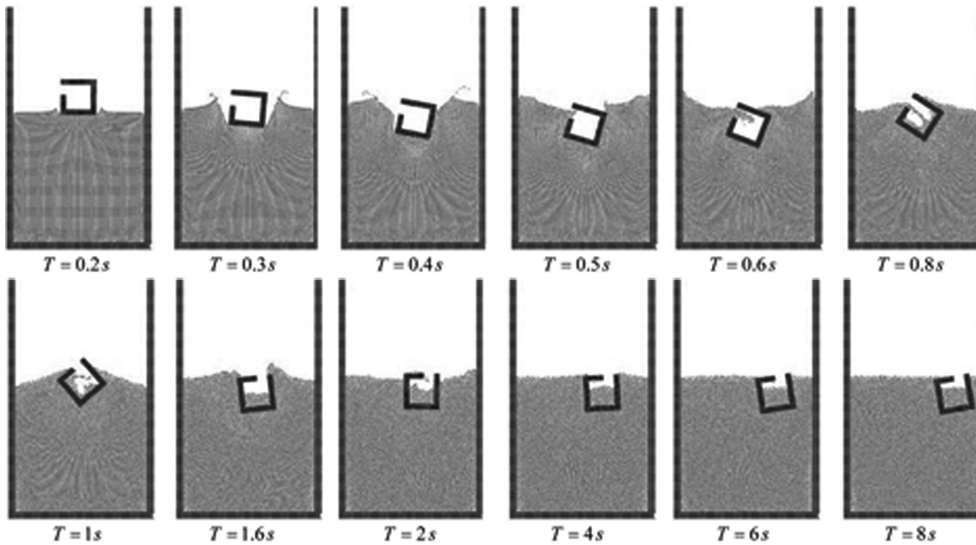


Fig. 4 Show the time history for free falling of Nylon vessel

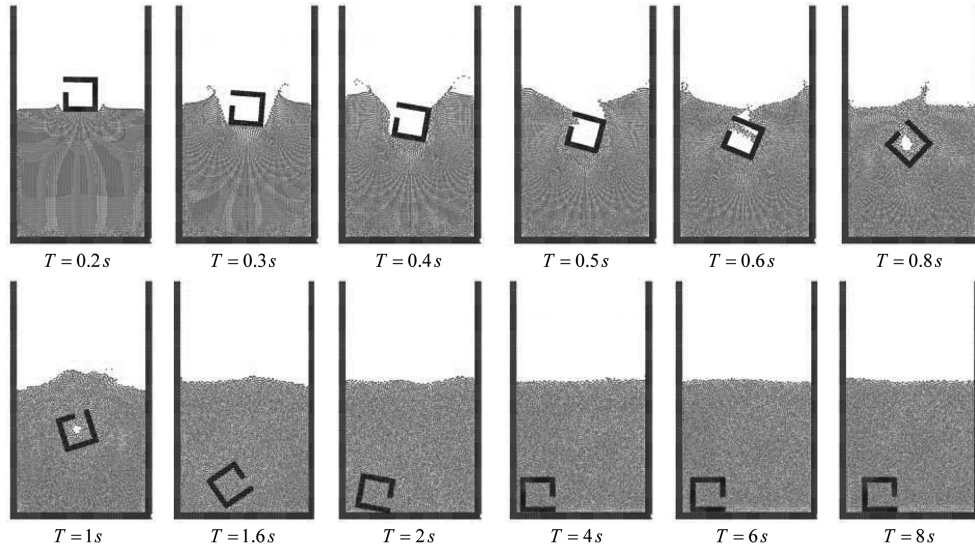


Fig. 5 Show the time history for free falling of Delrin vessel

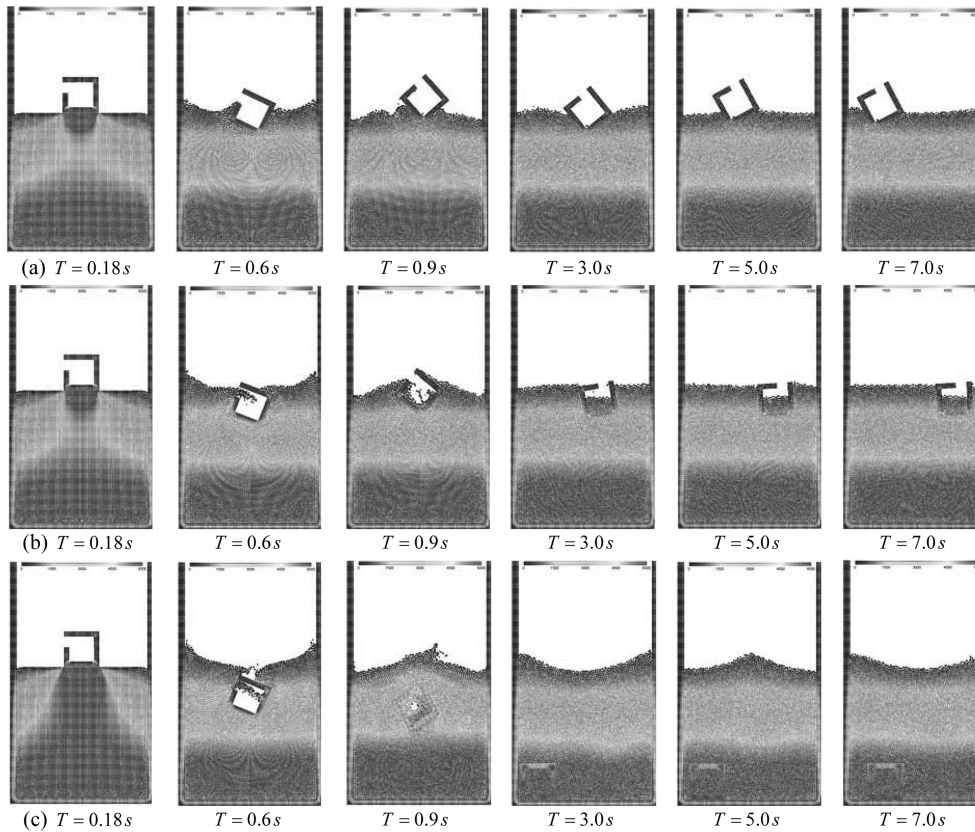


Fig. 6 Show the time history of pressure distribution during free falling of (a) Polypropylene vessel (b) Nylon vessel and (c) Delrin vessel, respectively

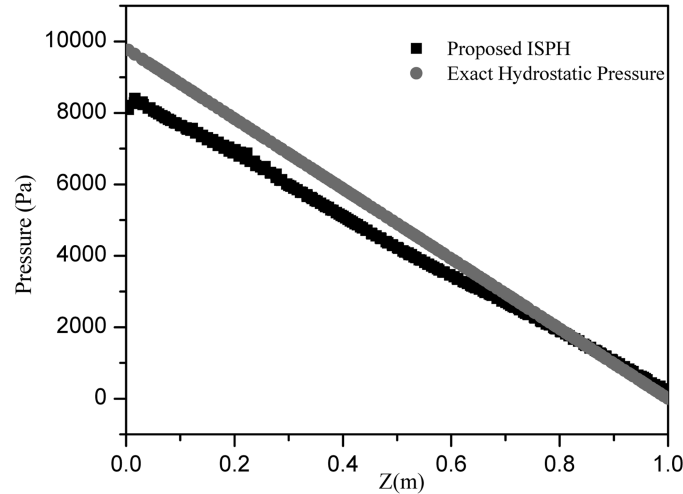


Fig. 7 Comparison between pressure values by proposed ISPH model and exact hydrostatic pressure at time 8.0 second

during the whole simulation. Due to the lack of experimental test related to the current simulation, the current simulation is compared only with the exact hydrostatic pressure as shown in fig. 7.

### 3.2 Water entry and exit of horizontal circular cylinder

In this section, we described the fully nonlinear free-surface deformations of initially calm water caused by the water entry and water exit of a horizontal circular cylinder with both free and forced vertical motions.

#### (a) Water entry with free motion

In this simulation, the deformation of free surface caused by dropped circular cylinder into calm water. The neutral buoyant and half buoyant circular cylinder with radius 5.5 cm are used in the calculations. ‘Neutrally buoyant’ means that the cylinder’s weight equals the buoyancy force on a totally submerged cylinder, while the ‘half buoyant’ means the cylinder’s weight equals one half of the buoyancy force. The relaxation coefficient in the current simulation is taken as ( $\alpha = 0.2$ ) and the time step  $\Delta t = 0.0005$  s.

The cylinder was dropped from the height of 50 cm between the lowest point of the cylinder and the mean free surface. Fig. 8 show the comparison of free surface deformation during water entry of circular cylinder between improved model and experimental results for Greenhow and Lin (1983) at the case of neutral buoyant. Also, Fig. 9 show the comparison of free surface deformation during water entry of circular cylinder between improved model and experimental results for Greenhow and Lin (1983) at the case of half buoyant. Note, the green color in the experimental snapshots is corresponds to BEM method for Sun and Faltinsen (2006). From these snapshots, a good agreement between the improved ISPH model, BEM method and experimental results has been found and the free surface has smoothness and small deformation in the improved model.

In addition, Fig. 10 shows the comparison of the depth penetration for the circular cylinder

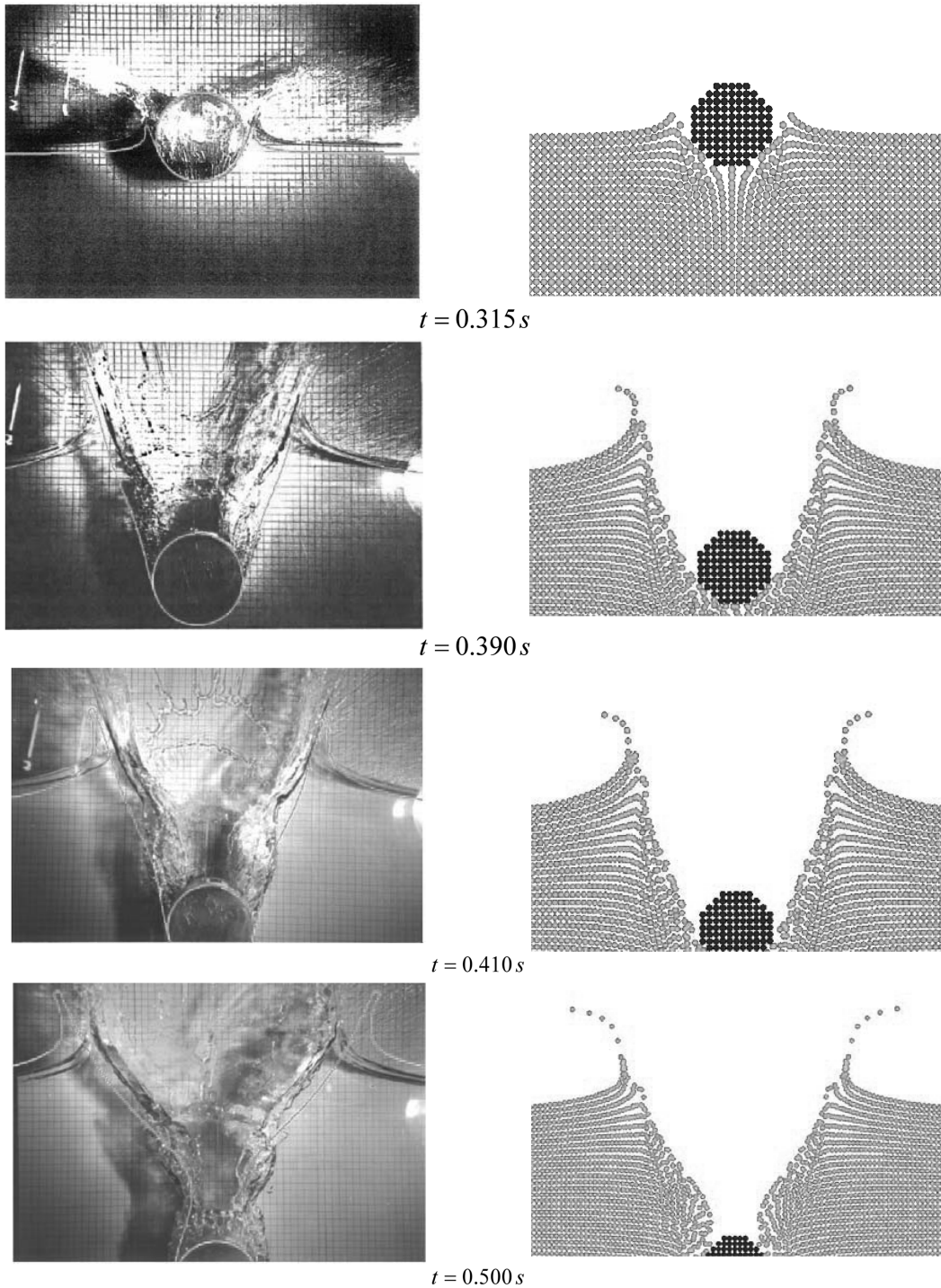


Fig. 8 Comparison of free surface deformation during water entry of circular cylinder between improved model (Right) and experimental results for Greenhow and Lin (1983) (Left) at the case of neutral buoyant.

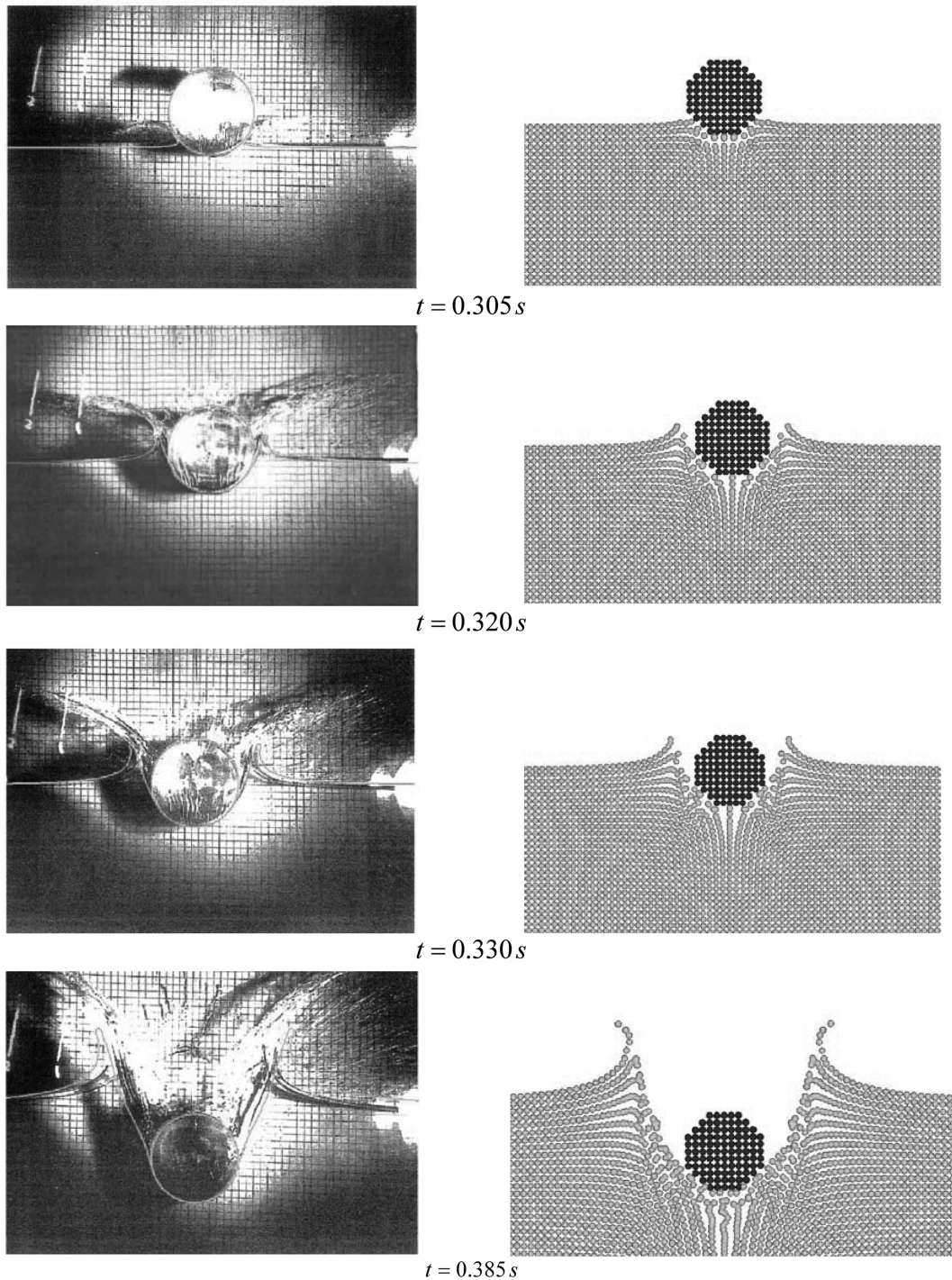


Fig. 9 Comparison of free surface deformation during water entry of circular cylinder between improved model (Right) and experimental results for Greenhow and Lin (1983) (Left) at the case of half buoyant.

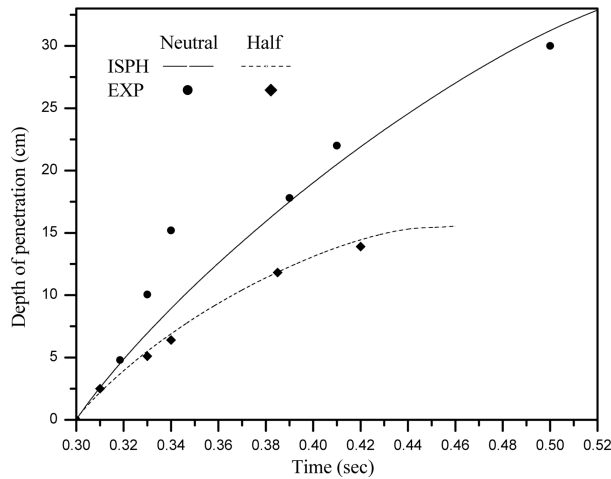


Fig. 10. Depth of penetration during water entry of neutral buoyant cylinder

between the improved ISPH model and experimental data as Greenhow and Lin (1983). It is clear that, from these comparisons, the improved model shows good agreement with experimental results for both two cases; neutral and half buoyant.

#### (b) Water exit of horizontal circular cylinder

The circular cylinder is rest at the bottom of the tank and is lifted by the constant force equal to the cylinder weight. The relaxation coefficient in the current simulation is taken as ( $\alpha = 0.2$ ) and the time step  $\Delta t = 0.0005$  s. Numerical results are compared with experimental results as Greenhow and Lin (1983). Fig. 11 shows the deformation in free surface during water exit of circular cylinder at several time instants, it is seen that, the water above the cylinder is lifted by the cylinder and thin layers of water are formed subsequently on the top of the cylinder and it falls down along the cylinder and causes breaking of the free surface. In addition, Fig. 12 shows the comparison of the distance from the top of the cylinder to mean free surface during water exit of a neutrally buoyant cylinder with experimental results as Greenhow and Lin (1983). It is observed that, the improved model shows relatively accurate result by comparing with the experimental results.

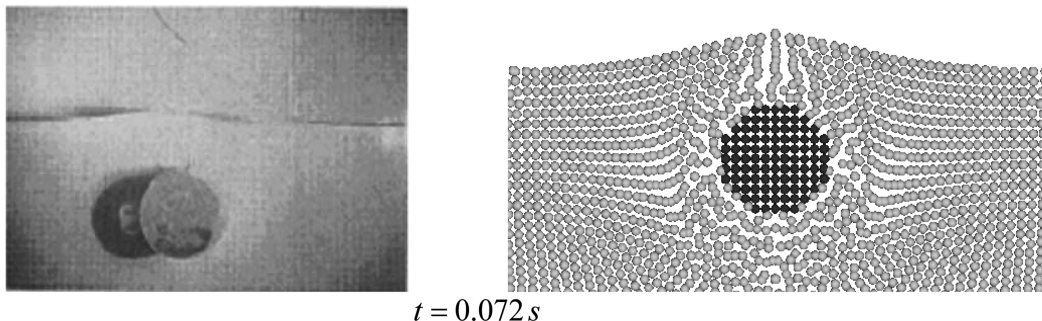


Fig. 11 Comparison of free surface deformation during water exit of circular cylinder between improved model (Right) and experimental results for Greenhow and Lin (1983) (Left)

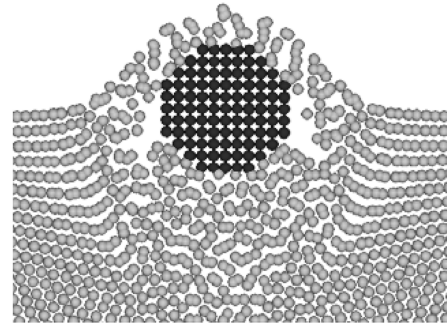
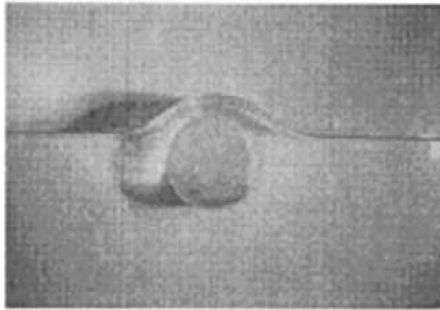
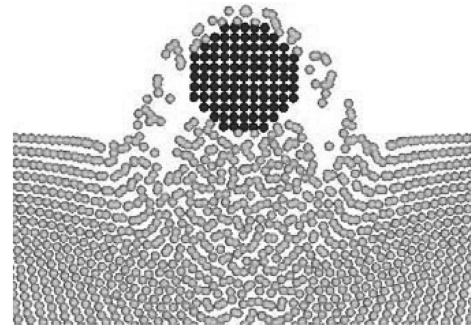
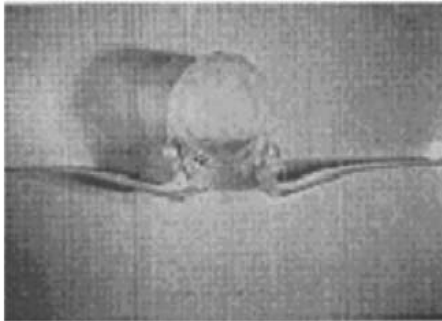
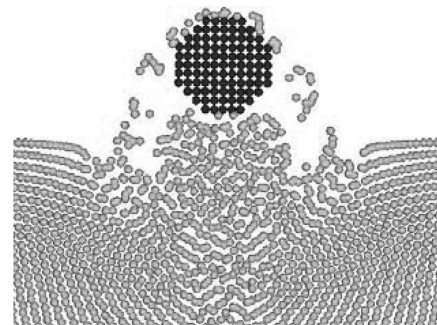
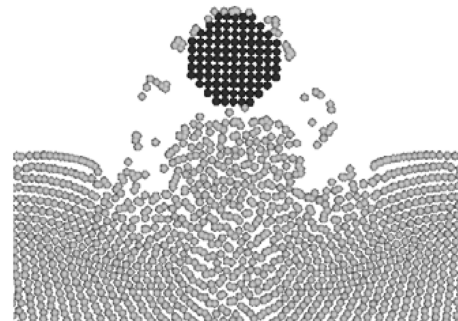
 $t = 0.165 s$  $t = 0.220 s$  $t = 0.248 s$  $t = 0.280 s$ 

Fig. 11 continued

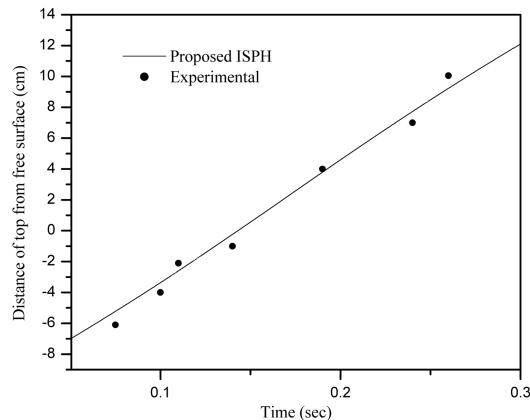


Fig. 12 The distance from the top of the cylinder to mean free surface during water exit of a neutrally buoyant cylinder

#### 4. Conclusions

A stabilized ISPH method is improved by introducing density invariance term with divergence of velocity term in the pressure Poisson equation. Also, the density invariance term is multiplied by relaxation coefficient for more stabilization. In this paper, the numerical simulations of the free falling vessels manufacturing from different materials have been performed. Moreover, water entry and water exit of horizontal circular cylinder have been performed by proposed incompressible SPH method.

In the water entry and exit of horizontal circular cylinder examples, the complicated free surface deformation is simulated with good agreement to the photographs taken from the experimental results. In addition, the depth of water penetration during water entry and the elapsed distance at water exit agree well with experimental results.

In this study, the improved ISPH method has many advantages such as:

- Keeping the total volume of fluid during the simulation which resultant from introduction of the density invariance term with a relaxation parameter into the source term of pressure Poisson equation.
- Preventing the penetration in rigid solid using suitable repulsive force which resultant from solving pressure Poisson equation for all dummy particles.
- Adjust the deformation in free surface by using reasonable eddy viscosity.

#### References

- Ellero M., Serrano, M. and Espanol, P. (2007), "Incompressible smoothed particle hydrodynamics", *J. Comput. Phys.*, **226**(2), 1731–1752.
- Gingold, R.A. and Monaghan, J.J. (1977), "Smoothed particle hydrodynamics: theory and application to nonspherical stars", *Mon. Not. R. Astron. Soc.*, **181**, 375–89.
- Gotoh, H., Sakai, T. (2006), "Key issues in the particle method for computation of wave breaking", *Coast. Eng.*, **53**(2-3), 171–179.
- Greenhow, M. and Lin W. (1983), "Non-linear free surface effects: experiments and theory", Report Number 83-

- 19, Department of Ocean Engineering, Massachusetts Institute of Technology.
- Greenhow, M. and Moyo, S. (1997), "Water entry and exit of horizontal circular cylinders", *Philos. T. R. Soc. A.*, **355**(1724), 551–563.
- Hirt, C.W. and Nichols, B.D. (1981), "Volume of fluid (VOF) method for dynamics of free boundaries", *J. Comput. Phys.*, **39**(1), 201–225.
- Hui, Sun and Odd, M. Faltinsen (2006), "Water impact of horizontal circular cylinders and cylindrical shells", *Appl. Ocean Res.*, **28** (5), 299–311.
- Khayyer, A., Gotoh, H. and Shao, S. (2008), "Corrected incompressible SPH method for accurate water-surface tracking in breaking waves", *Coast. Eng.*, **55**(3), 236–250.
- Khayyer, A., Gotoh, H. and Shao, S. (2009), "Enhanced predictions of wave impact pressure by improved incompressible SPH methods", *Appl. Ocean Res.*, **31**(2), 111–131.
- Kleefsman, K.M.T., Fekken, G., Veldman, A.E.P., Iwanowski, B. and Buchner, B. (2005), "A volume-of-fluid based simulation method for wave impact problems", *J. Comput. Phys.*, **206**(1), 363–393.
- Koshizuka, S., Nobe, A. and Oka, Y. (1998), "Numerical analysis of breaking waves using the moving particle semiimplicit method", *Int. J. Numer. Meth. Fl.*, **26**, 751–769.
- Koshizuka, S. and Oka, Y. (1996), "Moving-particle semi-implicit method for fragmentation of incompressible fluid", *Nucl. Sci. Eng.*, **123**(3), 421–434.
- Lee, E.S., Laurence, D., Stansby, P.K., Violeau, D. and Moulinec C. (2006), "2D flow past a square cylinder in a closed channel", *SPHERIC Newsletter*, No. 3.
- Lee, E.S., Moulinec, C., Xu, R., Violeau, D., Laurence, D. and Stansby P. (2008), "Comparisons of weakly compressible and truly incompressible algorithms for the SPH mesh free particle method", *J. Comput. Phys.*, **227** (18), 8417–8436.
- Lee, B.H., Park, J.C., Kim, M.H., Jung, S.J., Ryu, M.C. and Kim, Y.S. (2010), "Numerical simulation of impact loads using a particle method", *Ocean Eng.*, **37**(2-3), 164–173.
- Lin, P.Z. (2007), "A fixed-grid model for simulation of a moving body in free surface flows", *Comput. Fluids*, **36**(3), 549–561.
- Liu, H., Gong, K. and Wang, B.L. (2009), "Modelling water entry of a wedge by multiphase SPH method", *SPHERIC Newsletter*, No. 9.
- Lucy, L.B. (1977), "A numerical approach to the testing of the fusion process", *Astron J.*, **88**, 1013–24.
- Miyata, H. and Park, J.C. (1995), Chap.5, "Wave breaking simulation", In: (Ed. Rahman, M.), *Potential Flow of Fluids*, *Computational Mechanics Publications*, UK, 149– 176.
- Morris, J.P., Fox, P.J. and Zhu, Y. (1997), "Modeling Low Reynolds Number Incompressible Flows Using SPH", *J. Comput. Phys.*, **136**(1), 214–226.
- Oger, G., Doring, M., Alessandrini, B. and Ferrant, P. (2006), "Two-dimensional SPH simulations of wedge water entries", *J. Comput. Phys.*, **213**(2), 803–822.
- Panahi, R., Jahanbakhsh, E. and Seif, M.S. (2006), "Development of a VoF-fractional step solver for floating body motion simulation", *Appl. Ocean Res.*, **28**(3), 171–181.
- Shao, S.D. and Lo, E.Y.M. (2003), "Incompressible SPH method for simulating Newtonian and non-Newtonian flows with a free surface", *Adv. Water Resour.*, **26**(7), 787–800.
- Shao, S. (2009), "Incompressible SPH simulation of water entry of a free-falling object", *Int. J. Numer. Meth. Fl.*, **59**(1), 91–115.
- Sussman, M., Smereka, P. and Osher, S. (1994), "A level set approach for computing solutions to incompressible two-phase flow", *J. Comput. Phys.*, **114**, 146–159.
- Tanaka, M. and Masunaga, T. (2010), "Stabilization and smoothing of pressure in MPS method by Quasi-Compressibility", *J. Comput. Phys.*, **229**(11), 4279–4290.
- Tyvand, P. and Miloh, T. (1995), "Free-surface flow due to impulsive motion of a submerged circular cylinder", *J. Fluid Mech.*, **286**, 67–101.
- Violeau, D. and Issa, R. (2007), "Numerical modelling of complex turbulent free-surface flows with the SPH method: an overview", *Int. J. Numer. Meth. Fl.*, **53**(2), 277–304.
- Zhao, R., Faltinsen, O. and Aarsnes, J. (1997), "Water entry of arbitrary two-dimensional sections with and without flow separation", *Twenty-first Symposium on Naval Hydrodynamics*, Trondheim, Norway, 408–423.